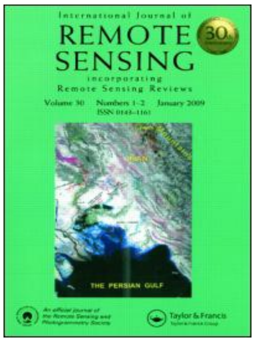

International Journal of Remote Sensing

ISSN: (Print) (Online) Journal homepage: https://www.tandfonline.com/loi/tres20

Examining phenological variation of on-year and off-year bamboo forests based on the vegetation and environment monitoring on a New Micro-Satellite (VENμS) time-series data

Longwei Li , Nan Li , Zhuo Zang , Dengsheng Lu , Guangxing Wang & Ni Wang

To cite this article: Longwei Li , Nan Li , Zhuo Zang , Dengsheng Lu , Guangxing Wang & Ni Wang (2021) Examining phenological variation of on-year and off-year bamboo forests based on the vegetation and environment monitoring on a New Micro-Satellite (VENμS) time-series data, International Journal of Remote Sensing, 42:6, 2203-2219, DOI: 10.1080/01431161.2020.1851802

To link to this article: https://doi.org/10.1080/01431161.2020.1851802

Published online: 30 Dec 2020.

INTERNATIONAL JOURNAL OF REMOTE SENSING
2021, VOL. 42, NO. 6, 2203–2219
https://doi.org/10.1080/01431161.2020.1851802

Examining phenological variation of on-year and off-year bamboo forests based on the vegetation and environment monitoring on a New Micro-Satellite (VENμS) time-series data

Longwei Li[a,b], Nan Li[a,b], Zhuo Zang[c], Dengsheng Lu[d,e], Guangxing Wang[f] and Ni Wang[a,b]

[a]School of Geographic Information and Tourism, Chuzhou University, Chuzhou, China; [b]Anhui Province Key Laboratory of Physical Geographical Environment, Chuzhou, China; [c]Research Center of Forest Remote Sensing & Information Engineering, Central South University of Forestry & Technology, Changsha, China; [d]Fujian Provincial Key Laboratory for Subtropical Resources and Environment, Fujian Normal University, Fuzhou, China; [e]School of Geographical Sciences, Fujian Normal University, Fuzhou, China; [f]Department of Geography and Environmental Resources, Southern Illinois University, Carbondale, IL, USA

ABSTRACT

Moso bamboo is an evergreen plant that extensively distributes in subtropical regions. Comparing to other forest types, Moso bamboo forest has some unique characteristics: high growth rate, short harvesting rotation, and on/off-year phenomenon. Plant phenology plays an important role in regulating carbon sequestration of the bamboo forest ecosystem. However, it is a challenge task to capture the phenological features of Moso bamboo forests on a regional scale due to frequent change of canopy structures and lack of high spatiotemporal remotely sensed data. The Vegetation and Environment monitoring on a New Micro-Satellite (VENμS) data with high spatiotemporal resolution provide the potential to examine the seasonal change of Moso bamboo forests. This research employs the VENμS time-series data (from January 2018 to December 2019) to analyse the spectral characteristics of on-year /off-year Moso bamboo forests and other two evergreen forest types (i.e., broadleaf forest and coniferous forest). The optimal spectral ranges for examining the seasonal variation of bamboo forests were determined. Three red-edge-based vegetation indices were reconstructed using the Harmonic analysis of time series (Hants) and compared. Red-edge position index (REPI) was selected to identify different phenological periods of Moso bamboo forests and other evergreen forest types. The results show that the spectral range of 730–920 nm in the VENμS data is sensitive to seasonal variation of Moso bamboo forests. The REPI can more effectively identify the two-year growing cycle of the bamboo forests than other vegetation indices, especially the bamboo shoots period. The start of the growing season of the off-year bamboo forest is approximately 50 to 60 days earlier than on-year bamboo forest. The results provided time-series phenological datasets of on-year and off-year Moso bamboo forests, which is valuable for local governments to conduct better ecological management and decision-making.

ARTICLE HISTORY
Received 18 August 2020
Accepted 28 October 2020

CONTACT Dengsheng Lu ludengsheng@fjnu.edu.cn Fujian Normal University, Cangshan Campus, No.8 Shangsan Road, Cangshan District, Fuzhou, Fujian, China 350007

1. Introduction

Moso bamboo forest extensively distributes in subtropical regions, accounting for 0.56% of the world's forest area (FAO 2014; Song et al. 2011), and has increasing trends both in areal expansion and logging products over the past three decades (Li et al. 2019; Yuen, Fung, and Ziegler 2017). It not only provides valuable goods and ecological services for the human community (Bai et al. 2016; Yuen, Fung, and Ziegler 2017), but also plays an important role in the carbon cycle and biodiversity of the subtropical forest ecosystem (Cao et al. 2019; Dai et al. 2018; Nath, Lal, and Das 2015; Yang et al. 2015). The potential carbon sequestration ability of Moso bamboo forest for mitigating climate change has caused widely attention (Cao et al. 2019; Dai et al. 2018; Yuen, Fung, and Ziegler 2017). Previous studies indicate that phenology is an important indicator of climate change and forest carbon cycle (Dannenberg et al. 2015; Liu et al. 2016; Melaas, Friedl, and Zhu 2013; Wu et al. 2017). Phenological characteristic is also valuable for bamboo forest mapping and aboveground biomass estimation (Chen et al. 2019; Henebry and de Beurs 2013; Li et al. 2019).

Remote sensing is an important tool for retrieval of the forest phenological characteristics. Remotely sensed time-series images such as moderate-resolution imaging spectroradiometer (MODIS) and Land Remote-Sensing Satellite (System, Landsat) are often used for examining land surface phenology (Melaas, Friedl, and Zhu 2013; Pastor-Guzman, Dash, and Atkinson 2018). Vegetation indices are commonly used in land surface phenology research because they have the potential to reveal phenological processes (Henebry and de Beurs 2013). For example, normalized difference vegetation index (NDVI) and enhanced vegetation index (EVI) are commonly used to indicate the phenological transitions of various forests (Guyon et al. 2011; Wu et al. 2014), including broadleaf or coniferous forests (Liu et al. 2016; Wu et al. 2014), and mangrove forests (Pastor-Guzman, Dash, and Atkinson 2018). Comparing to traditional vegetation indices based on red and near-infrared (NIR) bands, the red-edge band and its transformed index are more sensitive in reflecting vegetation growing status. For example, the red-edge position (REP), defined as the inflection point of red-NIR slope (Clevers et al. 2002), has strong correlations with chlorophyll and nitrogen (Clevers and Gitelson 2013; Main et al. 2011; Zarco-Tejada et al. 2019). Plants show bad growing condition when REP shifts to shortwave direction, and good condition when REP shifts to the longwave direction. Generally, the growing phenology of evergreen forests is difficult to monitor because the time series of vegetation indices have relatively small variation comparing with deciduous forests (Liu et al. 2016).

Time series of vegetation index dataset generated in the initial step includes various noise components; thus, smoothing methods are applied to time series of vegetation index dataset to minimize residual noise and reconstruct more representative vegetation condition. Methods for smoothing and reconstructing time-series data can be divided into three categories (Zeng et al. 2020): (1) empirical methods such as moving average filter (Ma and Veroustraete 2006) and changing-weight filter (Zhu et al. 2012), (2) curve fitting methods such as logistic models, improved logistic models; Elmore et al. 2012; Zhang et al. 2003), and Savitzky-Golay (Chen et al. 2004), (3) data transformation such as Fourier transforms (Hermance 2007) and wavelet analysis (Sakamoto et al. 2005). The time-series vegetation index is decomposed into a cyclical, trend, seasonal, and irregular (e.g. noise) components. Harmonic analysis of time series (Hants) is an improvement of fast Fourier transform (Zhu et al. 2015), which can remove noise points and does not need strict time-series intervals, thus, can process remote-sensing image data with different time intervals. Hants are flexible in the selection of frequency and time-series length.

Moso bamboo is an evergreen plant and has some unique phenological features comparing to other forest types (Fang et al. 2015; Li et al. 2019). For example, deciduous broadleaf forest has an obvious start of growing season and end of the growing season in a whole year. The unique nutrient circulation system of Moso bamboo forests produces the on-year and off-year phenomenon (Chen 2010). The on-year bamboo forests produce numerous new bamboo shoots in spring, while the off-year bamboo forests produce almost no bamboo shoots. Hence, the growing cycle and phonological features of Moso bamboo are different from other forests. The growing cycle of other evergreen forests (e.g., broadleaf and coniferous forests) is one year, while Moso bamboo forests have a two-year growing cycle. There are two growing periods (on-year and off-year), one leaf change period (off-year), one bamboo shoot growth period (on-year) and one bamboo rhizome growth period (off-year) in two years (Fang et al. 2015). These unique characteristics make the bamboo forest stand structures change in a whole year, and it is a challenge to examine its phenological feature by time-series Landsat and MODIS data. The Landsat data with 16 days revisit period cannot effectively capture its phenological features, while MODIS data have limited capability in monitoring the bamboo forest phenology because of its coarse spatial resolution (Chen et al. 2019). Due to the complex and frequent changes of bamboo forests, high-temporal remotely sensed data are needed for phenological analysis.

With the development of remote-sensing technology, more sensors with higher spatiotemporal resolutions are available. Satellites with red-edge bands can be used for vegetation phenology monitoring, such as Medium Resolution Imaging Spectrometer (MERIS), RapidEye, Worldview, and Sentinel-2. Vegetation and Environment monitoring on a New Micro-Satellite (VENμS), a near-polar sun-synchronous orbit microsatellite, was jointly developed by Israel Aerospace Agency (ISA) and French Centre National d'Etudes Spatiales (CNES), and was launched in August 2017 (Manivasagam, Kaplan, and Rozenstein 2019). This satellite provides multispectral bands covering visible, red-edge and NIR with a wavelength range of 443– 910 nm, revisit period of 2 days, and spatial resolution of 5 m. Comparing to the Landsat and Sentinel-2 data, although VENμS does not carry shortwave infrared spectral bands, its four red-edge bands may have the ability to accurately retrieve red-edge point (Frampton et al. 2013), and land surface phenological features (Herrmann et al. 2011; Xie et al. 2019). The dense time series of VENμS images and multiple red-edge bands may have the potential to retrieve the tiny phenological changes of bamboo forests while other sensor data cannot.

Our previous research demonstrated the importance of using red-edge bands and phenology information in the extraction of bamboo forest (Li et al. 2019), but its phenological change in two-year growth cycle has not been explored because of the relatively coarse temporal resolution of Landsat 8 and Sentinel-2 data and the cloud problems in subtropical regions. In this research, we obtained a dense time series of VENμS data between 2018 and 2019 which provided the opportunity to explore phenological features of bamboo forest. We will comparatively analyse spectral bands from visible to near-infrared to determine optimal bands for monitoring seasonal changes of Moso bamboo forests, propose several vegetation indices based on the red-edge scenarios (non-red-edge band, single red-edge band, and multiple red-edge bands), and then update each time-series vegetation index by Hants. We will also compare different phenological periods among on-year/off-year bamboo forest and other evergreen forests, and explore the influence of meteorological factors on the phenological features of Moso bamboo forests. This research can provide a better understanding of the phenological characteristics of bamboo forests. This information will be helpful for local governments to develop proper policies for better managing bamboo plantations and productions.

2. Materials and methods

2.1. Study area

The study area with a size of 54 km by 27 km (Figure 1(*a-b*)) is located at Anji County, Zhejiang Province, China, and has a mountain from northeast to southwest with an elevation range from 0 m to 1100 m (Figure 1(*c*)). This region belongs to subtropical monsoon climate with annual precipitation of 1512 mm and annual temperature of 16.9°C and has distinct seasons, that is, warm in spring, hot and humid in summer, cool in fall, cold and damp in winter (Chen et al. 2019). The main forest types include broadleaf, coniferous and bamboo forests.

Anji County is regarded as the 'hometown' of bamboo forests in China, and has the most widely distributed Moso bamboo forests which mainly distributed along the mountain with an altitude from 0 to 700 m and slopes of less than 40°. Moso bamboo forests play an important role in the economic condition in Anji County, and have enormous effects on food, construction, art, tourism and other industry. In 2015, the county's bamboo industry sale revenue was 5.36 billion yuan, accounting for 17.67% of the total gross domestic product in Anji County (Anji Forestry Bureau 2016). According to previous studies, Moso bamboo forests accounted for 48.7% of the total area in Anji County (Li et al. 2019).

2.2. Data collection and processing

The data sets used in this research included VENμS time-series imagery, field survey data, and Moso bamboo forest distribution map (Table 1). VENμS data with two days revisit period have 12 multispectral bands (wavelengths between 415 nm and 910 nm). A total of 87 VENμS images (Level-2 products, 10 m spatial resolution) between 2018 and 2019 were downloaded from Theia land data centre, and 59 images (list in Table 1) were selected in this study considering the cloud cover problem.

Atmospheric corrections were carried out using Multi-sensor Atmospheric Correction and Cloud Screening (MACCS) algorithm (Hagolle et al. 2008, 2010). The Bidirectional Reflectance Distribution Function (BRDF) correction was performed using the c-factor technique that uses global coefficients (Roy et al. 2016; Roy, Li, and Zhang 2017), and the BRDF coefficients of Sentinel-2 data were applied to VENμS data due to their similar spectral bands (Table 2), such as visible, red-edge and NIR bands. Nadir BRDF-adjusted reflectance values were derived for time-series VENμS data. The details of the adjust function and the parameters were provided by Manivasagam, Kaplan, and Rozenstein (2019). The cloud and shadow pixels in all images were masked out using the quality band. Seven adjusted spectral bands (Blue band, Green band, Red band, three red-edge bands and NIR band) were used in this study. Universal Transverse Mercator Projection (UTM 50) was selected for time-series VENμS data.

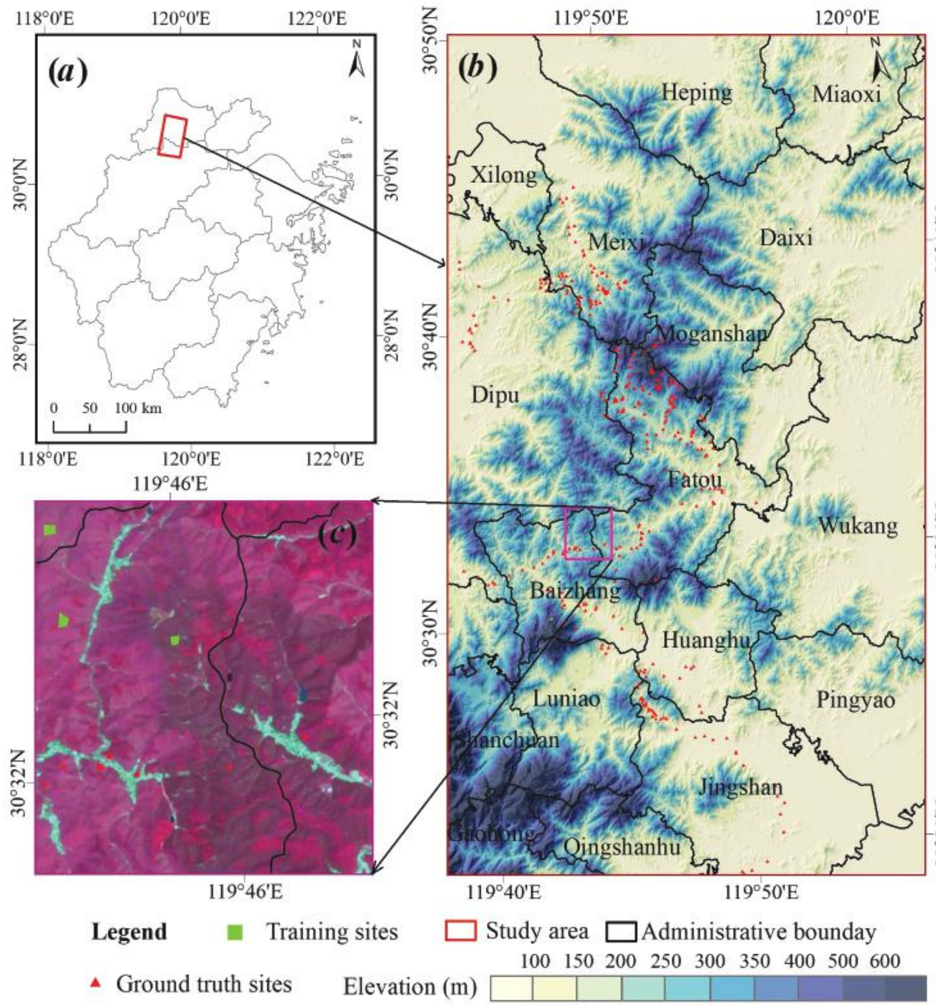

Figure 1. Location of the study area: (*a*) Northwest Zhejiang Province, China. (*b*) Study area. (*c*) False colour composites of VENµS data on 3 May 2018.

Table 1. Dataset used in this study.

Dataset	Acquisition date
VENµS images	6 February 2018, 8 February 2018, 12 February 2018, 26 February 2018, 28 March 2018, 3 April 2018, 9 April 2018, 11 April 2018, 15 April 2018, 17 April 2018, 29 April 2018, 3 May 2018, 14 June 2018, 18 June 2018, 26 June 2018, 10 July 2018, 14 July 2018, 26 July 2018, 28 July 2018, 5 August 2018, 7 August 2018, 23 August 2018, 29 August 2018, 28 October 2018, 30 October 2018, 1 November 2018, 9 November 2018, 23 November 2018, 27 November 2018, 1 December 2018, 17 December 2018, 29 December 2018,18 January 2019, 22 January 2019, 24 January 2019, 23 March 2019, 6 April 2019, 8 April 2019, 4 May 2019, 14 May 2019, 22 May 2019, 28 May 2019, 3 June 2019, 5 June 2019, 29 July 2019, 2 August 2019, 30 August 2019, 23 September 2019, 25 September 2019, 29 October 2019, 31 October 2019, 14 November 2019, 20 November 2019, 8 December 2019, 10 December 2019, 12 December 2019, 14 December 2019, 16 December 2019, 28 December 2019,
Field survey data	In 2018 and 2019, field survey data including on-year/off-year bamboo forest and other land cover types were collected.
Auxiliary data	The meteorological data include daily precipitation (mm), daily maximum temperature, daily minimum temperature and daily average temperature between 2018 and 2019.

Table 2. Spectral bands of VENμS and BRDF model coefficients used in this study.

Band name	Central wavelength (nm)	Band width (nm)	Spatial resolution (m)	f_{iso}	f_{geo}	f_{vol}
B_3, Blue	492	40	10	0.0774	0.0079	0.0372
B_4, Green	555	40	10	0.1306	0.0178	0.0580
B_7, Red	666	40	10	0.1690	0.0227	0.0574
B_8, Red-edge1	702	40	10	0.2085	0.0256	0.0845
B_9, Red-edge2	741	40	10	0.2316	0.0273	0.1003
B_{10}, Red-edge3	782	30	10	0.2599	0.0294	0.1197
B_{11}, NIR	861	16	10	0.3093	0.0330	0.1535

f_{iso}, f_{vol} and f_{geo} are the constant values of BRDF spectral model parameters.

Field work was conducted in 2018 and 2019. Ground truth land cover data and Moso bamboo phenological information were recorded (Figure 1(*c*)). According to the field survey, polygons of typical forest types in the study area were sketched on Google Earth. A total of 359 polygons (Figure 1(*c*)) were selected as the training samples for time-series spectral analysis, including 95 plots (640 pixels) of off-year bamboo forests, 86 plots (540 pixels) of on-year bamboo forests, 48 plots (358 pixels) of coniferous forests and 60 plots (253 pixels) of broadleaf forests. All polygons were checked to make sure there were no clouds and shadows in the time series of VENμS data.

2.3. Time-series spectral analysis of Moso bamboo forest

Based on field survey data and high-resolution satellite images, the collected plots were checked to make sure that no land cover change occurred during the period between 2018 and 2019. The average spectral reflectance value of each forest type was calculated, and the spectral curves of on-year/off-year bamboo forests, coniferous and broadleaf forests were developed, respectively. The spectral range for seasonal change was determined based on comparative analysis of time-series spectral bands.

2.4. Comparative analysis of time-series vegetation indexes

Based on spectral analysis from visible to NIR bands, three scenarios – non-red-edge band (NDVI, EVI), a single red-edge band ($NDVI_{red-edge702}$) and multiple red-edge bands (REPI) (see Table 3) were selected to comparatively analyse the phenological features of Moso bamboo forests and other forest types.

In order to reduce the impact of noise on data analysis, Hants was used to filter and smooth the time series of vegetation index data. Hants combine filtering and smoothing methods, make full use of the spatiotemporal characteristics of remote-sensing images and take the reconstruction of time-series images into the periodicity of vegetation growth. The vegetation index (such as NDVI) is reconstructed by combining the vegetation frequency curves of different growth periods. The Hants can be expressed as Equation (1):

$$\mathrm{VIs}(t_j) = a_0 + \sum_{i=1}^{N}\left(a_i \cos\left(\frac{2\pi}{L}t_j\right) + b_i \sin\left(\frac{2\pi}{L}t_j\right)\right) \tag{1}$$

Table 3. Vegetation indices used in this research.

Scenario	Vegetation index	Formula	Source
Non-red-edge index	Normalized Difference Vegetation Index (NDVI)	$\frac{(NIR)-(Red)}{(NIR)+(Red)}$	(Tucker 1979)
	Enhanced Vegetation Index (EVI)	$\frac{2.5\times((NIR)-(Red))}{(NIR)+6\times(Red)-7.5\times(Blue)+1}$	(Liu and Huete 1995)
Single red-edge index	Normalized Difference Vegetation Index based on red-edge ($NDVI_{red\text{-}edge}$)	$\frac{(NIR)-(Red-edge_{702})}{(NIR)+(Red-edge_{702})}$	(Fernández-Manso, Fernández-Manso, and Quintano 2016)
Multiple red-edge index	Red-edge Position Index (REPI)	$\frac{\left(\frac{(Red)+(Red-edge_{782})}{2}-(Red-edge_{702})\right)}{(Red-edge_{742})-(Red-edge_{702})}$	(Clevers et al. 2002)

Note: NIR and Red represent near infrared (865 nm) and Red band (650 nm); Red-edge$_{702}$, Red-edge$_{742}$ and Red-edge$_{782}$ represent Red-edge spectral bands in wavelengths of 702 nm, 742 nm and 782 nm, respectively.

Where VIs(t_j) is the modelled vegetation index value for a single-pixel location; a_0 is the Fourier coefficient, a_i and b_i are Fourier coefficients for harmonic component i with $N \geq 1$ components; L is the length of the time period, and set to 730 in this study; and t is time and set as the day of the year between 2018 and 2019 of each VENμS acquisition.

Based on field survey, the bamboo forest phenological periods were grouped as different colours, which matched with REPI time-series data in two-year cycle. For example, the bamboo shoots period in on-year bamboo forests was set as blue colour, and the leaf-changing period in off-year bamboo forests was set as a yellow colour. The phenological characteristics such as the start of the growing season were compared between on-year and off-year bamboo forests. In addition, precipitation and temperature data were also included in analysing their impacts on time-series REPI. Cumulative data of temperature and precipitation are calculated to correlate with time-series REPI, time points 1, 5, 8, 13, 21, 34, 55, and 89 days were selected for calculation. For example, the 5 days cumulative precipitation refers to the total precipitation in the past 5 days, and this 5-day cumulative precipitation was analysed with time-series REPI by correlation analysis. The correlation coefficient r is used to indicate their correlation.

3. Results

3.1. Time-series spectral characteristics of on-year and off-year bamboo forests

The comparative analysis of time-series spectral curves (Figure 2) indicates that the B_9, B_{10} and B_{11} bands have obvious spectral variation in 1 year (the value range is from 0.15 to 0.55) and the reflectance of these four bands increased in spring and decreased in fall, while other bands (B_3, B_4, B_7 and B_8) have a small range (between 0 and 0.13) with a relatively stable trend in a whole year. The difference in seven spectral bands demonstrated that red-edge (B_9, B_{10}) and NIR (B_{11}) bands had higher seasonal variation than other spectral bands, implying that the spectral bands between 730 nm and 920 nm have the potential for better discriminating seasonal variations of different forest types.

On-year and off-year bamboo forests showed different phenological change patterns comparing to other two evergreen forest types. The dates of increasing spectral values vary between off-year and on-year bamboo forests (Figure 2(*a*) vs Figure 2(*b*)). For example, the date of increasing spectral value in band 9 (red-edge band between 734 nm and 750 nm, red circle in Figure 2) is near 110 (Figure 2(*a*)) for off-year bamboo, while it is near 130 for on-

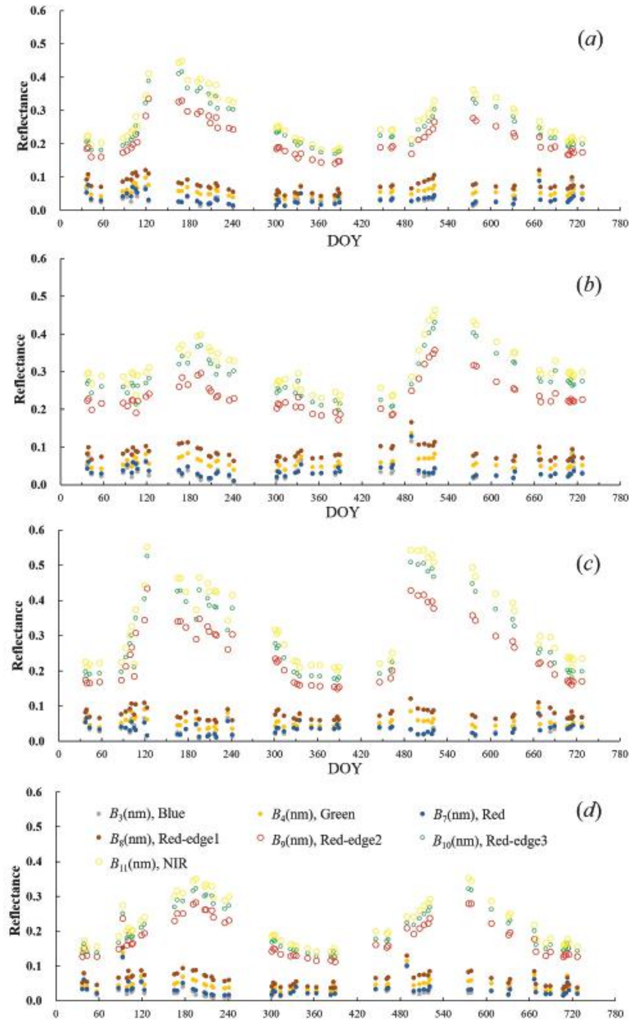

Figure 2. Time-series spectral variations of evergreen forest types in VENμS multispectral data between January 2018 and December 2019. (*a*) off-year bamboo; (*b*) on-year bamboo; (*c*) broadleaf forest; (*d*) coniferous forest).

year bamboo (Figure 2(*b*)). This difference of spectral increase is related to the start of the growing season of Moso bamboo forest, and proved valuable for effectively distinguishing on-year and off-year bamboo forests (Chen et al. 2019; Li et al. 2019). The dates of increasing values for a coniferous forest are the same as off-year bamboo forest, but the broadleaf forest has earlier dates than other forest types, it is near 100. In addition, the peak values of these evergreen forest types vary. For instance, broadleaf and coniferous forests have peak values of near 0.60 and 0.38, respectively, while off-year and on-year bamboo forests have peak values of near 0.48.

One interesting thing is that the peak values of bamboo forests between 2018 and 2019 vary, comparing to other forest types. For example, the peak value of off-year bamboo is near 0.48 in 2018 and 0.38 in 2019. This phenomenon demonstrated that the Moso bamboo forests have different growing conditions within 2 years. Although the spectral values of these evergreen forest types show different trends within 2 years, it is necessary to identify the sensitive band combination (e.g. NDVI, EVI, $NDVI_{red\text{-}edge702}$) and to conduct comparative analysis for distinguishing phenological characteristics of these evergreen forest types.

3.2. Comparative analysis of time-series vegetation indices

The time-series vegetation indices of four evergreen forest types (Figure 3) have dramatic increased values after a day of the year (DOY) 100, and declined values after DOY 270, indicating their starts or ends of growing seasons. The time-series trends of off-year bamboo forests are similar to broadleaf and coniferous forests, while on-year bamboo forests show a downward trend in early 2018.

The smoothing effects of time-series vegetation indices are obviously different. For example, the NDVI values of bamboo forests and coniferous forests are concentrated on 0.70–0.90, while broadleaf forests are on 0.60–0.95. The fitting effect of NDVI $_{red\text{-}edge702}$ is close to NDVI. NDVI and $NDVI_{red\text{-}edge702}$ have a weak ability to separate the seasonal difference of on-year and off-year bamboo forests. In contrast, the difference of time-series EVI among four forest types is obvious. The time-series EVI values of bamboo forests are concentrated on 0.40 to 0.70, the broadleaf and coniferous forests are on 0.40–0.80 and 0.20–0.60, respectively. The fitting effect of time-series EVI is better than that of NDVI

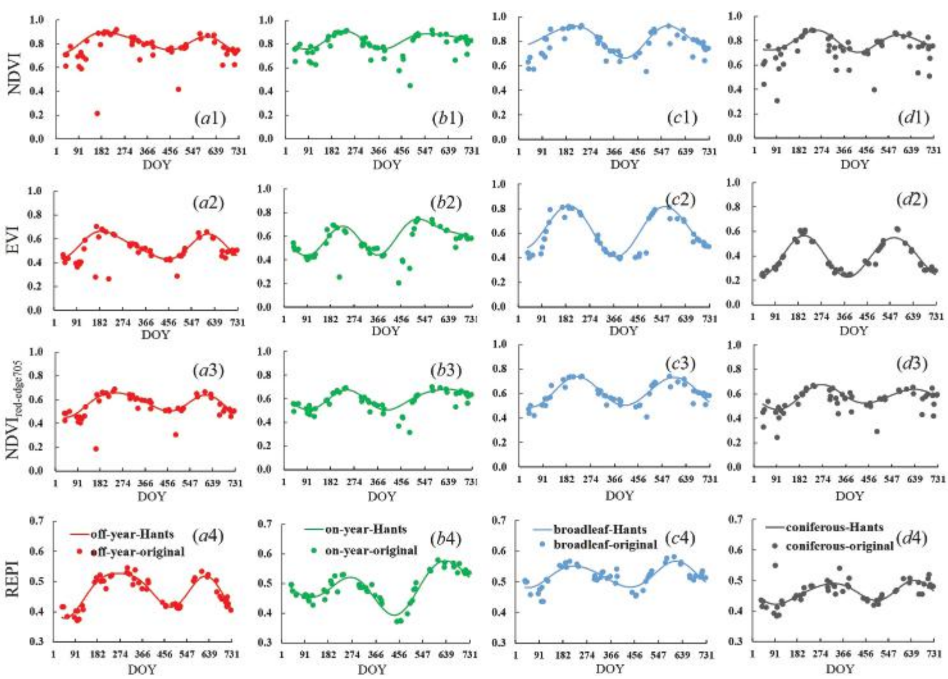

Figure 3. Comparison of time-series vegetation indices of on-year/off-year bamboo forests and other evergreen forest types. Series (*a*1)–(*a*4), (*b*1)–(*b*4), (*c*1)–(*c*4) and (*d*1)–*d*4) represent four vegetation indices of off-year bamboo forests, on-year bamboo forests, broadleaf forests and coniferous forests.

and NDVI $_{red\text{-}edge702}$. EVI can distinguish the spring changes of on-year and off-year bamboo forests, and the periodic changes of on-year and off-year bamboo forests.

The fitting curve of REPI, compared with those of NDVI, NDVI $_{red\text{-}edge702}$ and EVI, has some differences, especially in the on-year bamboo forest. There is an obvious valley at the 456 day (March of the second year), which corresponds to leaf change period of the Moso bamboo forest, while the NDVI, NDVI $_{red\text{-}edge702}$ and EVI have many values distributed at this time; however, they have not been fitted, and their fitted times are significantly earlier than 456 days. Comparing the performance of all four time-series indexes, REPI can not only show the difference in the growth cycle of the bamboo forest, for instance, the index peak value of the off-year is greater than that of the on-year, but also distinguish the specific phenological period of the on-year and off-year bamboo forests, such as the leaf change period.

The comparison of three red-edge band scenarios and the phenological change characteristics indicates that REPI showed relative better fitting performance. For example, from DOY 1 to DOY 120, there is leaf-change period for off-year bamboo forests and bamboo shoots periods for on-year bamboo forests. Figure 3(b4) shows that REPI reflects the downward trend of the on-year bamboo forest in the spring (the REPI value is still higher than 0.4); meanwhile, the REPI reflects a downward trend of off-year bamboo forests (the REPI value is lower than 0.4) (Figure 3(b4), DOY456). The reason for the difference is that the REPI shows low values in the leaf change for the off-year bamboo forests, and the REPI keeps higher in the bamboo shoots for the on-year bamboo forests. The REPI of an on-year bamboo forest shows downward because new bamboo shoots have no leaf in this period, the nutrition is transported by an on-year old bamboo tree, and the colour of old bamboo tree leaves turns to yellow, thus REPI decreased. Hence, REPI is selected for comparative analysis of the phenological difference between bamboo forests and other evergreen forest types.

3.3. Analysis of the phenological variations of the Moso bamboo forests

The time-series REPI shows that broadleaf and coniferous forests have the same growing cycles between 2018 and 2019, confirming their one-year growing cycle, but on-year and off-year bamboo forests presented different growing cycles and patterns. In a two-year cycle of Moso bamboo forests, the leaf change period (yellow in Figure 4), bamboo rhizome growth period (grey), and bamboo shoot period (blue) occur at one time, and bamboo growing period (green) occur at two times.

The obvious difference between off-year and on-year bamboo forests is the start of the growing season, that is, off-year bamboo forests start to grow after leaf change period (approximately at 90 days, Figure 4(c3)), and on-year bamboo forests after the bamboo shoots period (approximately at 150 days, Figure 4(c2)). Hence, the start growing season of off-year bamboo forests is about 50–60 days earlier than on-year bamboo forests. From 90 to 150 days, Figure 4(c1-c4) shows that the new bamboo trees start to develop new leaves.

Temperature and moisture are important factors influencing the start, magnitude, and end of growing seasons. Figure 4(*d*) confirms the close relationships between the growth of bamboo forests with temperature and precipitation. The time-series REPI shows a lagging trend with temperature, especially in 2018, and the REPI peak lags behind the time-series temperature data. Table 4 showed that cumulative temperature is correlated

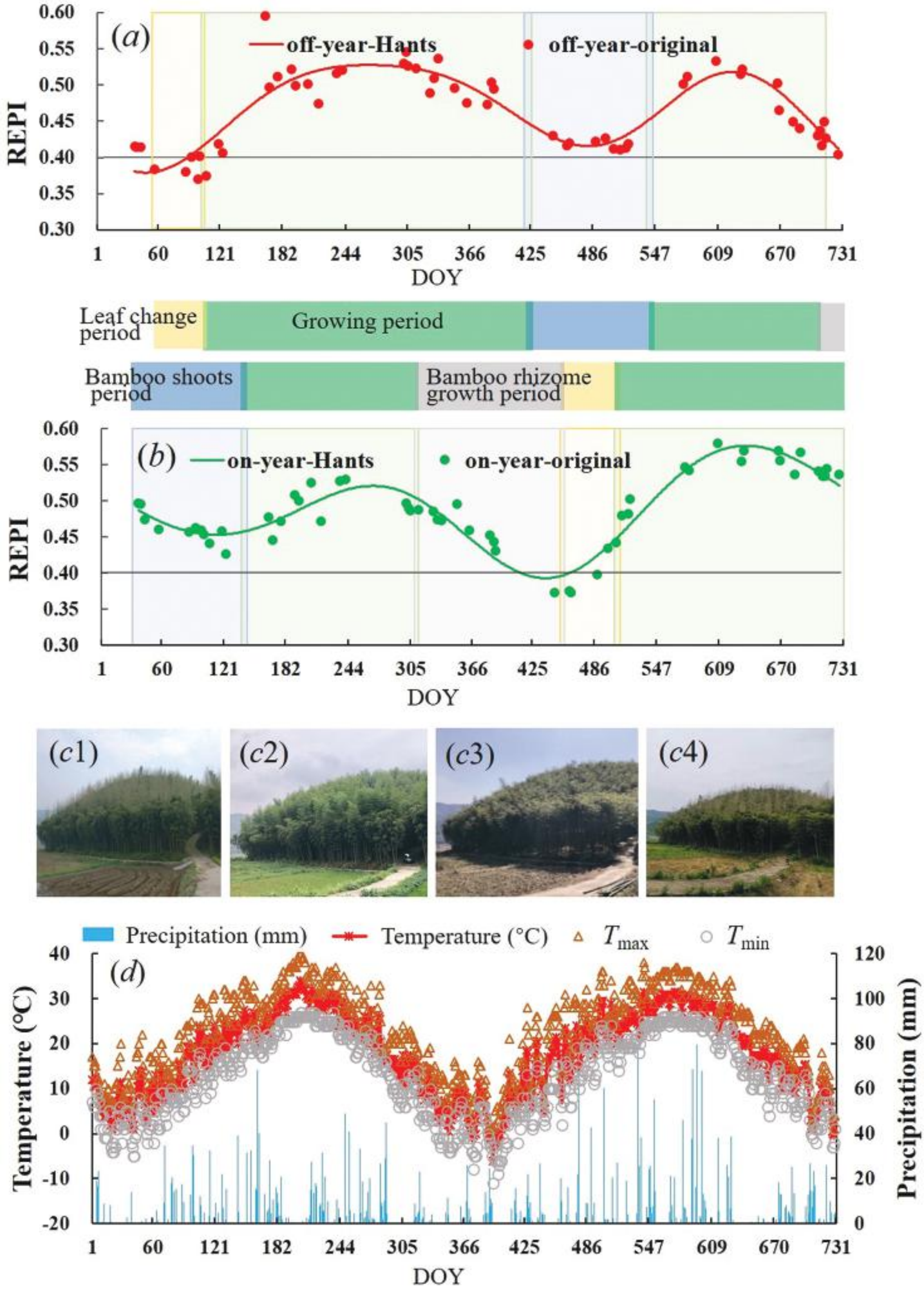

Figure 4. The seasonal change of on-year/off-year Moso bamboo forests and other evergreen forest types. (*a*) and (*b*) represent time-series REPI of off-year and on-year bamboo forests. Yellow, Green, Grey, and Blue ramp represent leaf change period, growing period, bamboo rhizome growth period and bamboo shoots period. (*c*1), (*c*2), (*c*3) and (*c*4) are pictures obtained on 25 May 2018, 2 August 2018, 12 March 2019 and 27 May 2020. (*d*) represent precipitation and temperature between 2018 and 2019.

Table 4. Correlation coefficient between REPI and cumulative temperature and precipitation data.

	The correlation coefficient *r* under different day							
	1	5	8	13	21	34	55	89
Cumulative temperature	0.21	0.24	0.28	0.31	0.38	0.46	0.58	0.74
Cumulative precipitation	−0.02	−0.03	−0.02	−0.01	0.01	0.11	0.31	0.58

with time-series REPI, especially the temperature. This correlation increases gradually with cumulative time, and the correlation coefficient reaches 0.74 as the cumulative time is 89 days. Meanwhile, the cumulative precipitation has a low correlation with REPI when cumulative time is less than 34 days, and it has a relatively high correlation especially when cumulative time reaches 89 days.

4. Discussion

4.1. Seasonal variation of Moso bamboo and implication in forest management

The phenological difference between off-year and on-year bamboo forests is caused by the photosynthesis process, chlorophyll content and nutrient cycling (Chen 2010). For example, the start of the growing season for an off-year bamboo forest is earlier than that of on-year bamboo forest. There is no leaf change of on-year bamboo forests because their leaves need to keep dark green, and to transfer nutrition to the new bamboo shoots in the spring. The leaves of new bamboo trees develop in June when the growing season of on-year bamboo begins. The off-year bamboo forests have almost no bamboo shoots in spring, and their leaves change between March and April (Fang et al. 2015; Zheng and Hong 1998) when the growing season of off-year bamboo begins. This growing difference between on-year and off-year bamboo forests is confirmed in previous studies (Chen et al. 2018; Xu et al. 2018; Zhou et al. 2019). After the growing season, the leaves of the off-year bamboo forest would keep green and store energy for the new bamboo shoots coming out in the next year, while the leaves of on-year bamboo forests gradually changed from green to yellow, because the bamboo rhizome growth consumes lots of nutrition, and the leaves fall down and change in the next spring.

The phenological characteristics of Moso bamboo forests also relate to human-induced management manners. For example, local farmers practice bamboo forest management according to the colour change of Moso bamboo trees. Few bamboo shoots occur in spring when the leaves of bamboo forests show yellow green (off-year bamboo forest), while plenty of bamboo shoots occur in spring when the leaves of bamboo trees are dark green (on-year bamboo forest). According to the colour of on/off-year bamboo forests, all bamboo shoots developed in off-year bamboo forests would be dug out by local farmers, while the bamboo shoots developed in on-year bamboo forests were kept to grow to bamboo trees. These management manners intensified the phenomenon of on-year and off-year.

4.2. Potential data and index for examining Moso bamboo phenology

The temporal resolution of remote-sensing data are an important consideration in the study of phenology due to the frequent changes of Moso bamboo forest in its 2-year growing stage. Landsat data with 16 days temporal resolution have many limitations in phenological research because phenological changes of Moso bamboo forests occur more rapidly than the 16 days revisit time and cloud cover problem reduces the number of Landsat images available (Zeng et al. 2020). In comparison, MODIS data with the daily temporal resolution are widely used for examining land surface phenology (Xu et al. 2018; Zhou et al. 2019). However, the mixed pixel problem caused by coarse spatial resolution results in many uncertainties and difficulty in identifying phenological features of a specific vegetation type. Another important factor in phenology study is the spectral resolution and the derived index. The spectral ranges from 730 to 920 nm, especial the red-edge spectral bands, have the potential to discriminate seasonal variation in evergreen forest types, but not all satellite sensors contain red-edge bands. For example, Landsat has only one NIR band in the sensitive spectral range.

Considering the sensor data availability and index portability, this study developed non-red-edge index (suitable for Landsat imagery) and multiple-red-edge index (suitable for Sentinel-2 and VENμS) for comparative analysis. Non-red-edge index (e.g. NDVI, EVI) can reflect some basic phenological characteristics of bamboo forests, such as start and end of growing seasons. EVI has a better performance than NDVI in representing the spring phenological features. This study indicated that vegetation indices based on red-edge bands had better performance than non-red-edge-based vegetation indices. REPI is able to show the leaf conditions in different phenological periods, especially in fall and winter. Comparing to REPI, other vegetation indices are difficult to reflect the unique features of bamboo forests, such as an off-year bamboo forest with dark green colour in winter and on-year bamboo forest with yellow-green colour. EVI could be transferred to Landsat series data, and REPI could be transferred to Sentinel-2 data. VENμS data with 5 m spatial resolution and 2 days revisit time are valuable for examining phenological features in Moso bamboo forests. The results in this research provide new insights for selecting suitable vegetation indices and image acquisition dates for examining on-year and off-year bamboo forest phenological features.

In addition to the impact of remote-sensing data, the data smoothing methods are expected to remove the noise component and maintain the integrity of vegetation dynamics. Smoothing the time-series vegetation indices with local windows can capture the vegetation dynamics better, but it is often sensitive to local fluctuation and data noise. Compared with a fitting method based on local windows, methods based on entire annual time series and harmonic series can get a smoother curve, but the problem that smoothing curve deviates from actual vegetation growth trajectory still may occur. This study fully considered the physiological and ecological characteristics of Moso bamboo forests, such as two-year growing stage. Hants were selected as the smoothing method, and the leaf-off period of off-year bamboo forests was captured and fitted. Phenological metrics extraction methods need to be selected based on more ground truth data of phenological features.

4.3. Research deficiency and improvement for future studies

This study analysed the potential spectrum and vegetation index in the study of Moso bamboo phenology. The high revisit frequencies of VENμS data could be captured theoretically at every 2 days. However, there are only 59 images between 2018 and 2019 can be used for time-series analysis due to excessive cloudiness in subtropical regions. Data gap is a big challenge for phonological retrieval. There are two ways to solve this problem, one is the combination of different sensor data to generate time-series data with high spatial and temporal resolutions, for example, Sentinel-2 data with 10–20 m spatial resolution and 5 days revisit and VENμS could be combined into one time-series by transformation model (Manivasagam, Kaplan, and Rozenstein 2019), which facilitates temporally dense Moso bamboo monitoring. In addition, the Unmanned Aerial Vehicle (UAV) could provide a data bridge between remote sensing and ground survey. The UAV data can also assist the phenological verification data, provide stable and reliable real phenological data, and improve the accuracy of the phenology of the bamboo forest. The other way is to improve the data filling method. The data filling method can be used to combine the features of the time series and the surrounding pixels to fill in missing pixels (Yan and Roy 2018) to improve the time resolution of the data.

5. Conclusions

Moso bamboo forests have frequent canopy structure change and unique phenological features compared with other forest types. The VENμS time-series data (5 m spatial resolution and 2 days revisit cycle) can effectively capture phenological characteristics of on-year/off-year bamboo forests. This research shows that the spectral bands between 730 and 920 nm wavelengths in VENμS data, especially the red-edge bands, have the potential to capture the bamboo forest phenological features. Based on the comparative analysis of phenological retrieval performances among different vegetation indices, multiple-red-edge indices have advantages over non-red-edge indices. The REPI based on multiple-red-edge bands can identify the frequent canopy changes and growing cycle of the bamboo forests, especially the bamboo shoots period between on-year and off-year bamboo forest in spring and fall. The start of the growing season of the off-year bamboo forest is earlier (approximately 50–60 days) than that of on-year bamboo forest. The results in this research can be used for local governments and farmers to make a better decision for bamboo forest management.

Acknowledgements

The time-series VENμS data were provided by Israel Aerospace Agency (ISA) and French Centre National d'Etudes Spatiales (CNES).

Disclosure statement

No potential conflict of interest was reported by the authors.

Funding

This research is financially supported by Zhejiang Provincial Natural Science Foundation [grant# LQ19D010010], China Scholarship Council [grant# 201808330382], and the Zhejiang A&F University's Research and Development Fund [Grant No. 2013FR052].

ORCID

Dengsheng Lu http://orcid.org/0000-0003-4767-5710

References

Anji Forestry Bureau. 2016. "Anji County Forestry Resources Survey Results Report". Anji, China: Anji Forestry Bureau.

Bai, S., Y. Wang, R. T. Conant, G. Zhou, Y. Xu, N. Wang, F. Fang, et al. 2016. "Can Native Clonal Moso Bamboo Encroach on Adjacent Natural Forest without Human Intervention?" *Scientific Reports* 6: 31504. doi:10.1038/srep31504.

Cao, L., C. N. Coops, Y. Sun, H. Ruan, G. Wang, J. Dai, and G. She. 2019. "Estimating Canopy Structure and Biomass in Bamboo Forests Using Airborne LiDAR Data." *ISPRS Journal of Photogrammetry and Remote Sensing* 148: 114–129. doi:10.1016/j.isprsjprs.2018.12.006.

Chen, J., P. Jönsson, M. Tamura, Z. Gu, B. Matsushita, and L. Eklundh. 2004. "A Simple Method for Reconstructing A High-quality NDVI Time-series Data Set Based on the Savitzky–Golay filter." *Remote Sensing of Environment* 91: 332–344. doi:10.1016/j.rse.2004.03.014.

Chen, S., H. Jiang, Z. Cai, X. Zhou, and C. Peng. 2018. "The Response of the Net Primary Production of Moso Bamboo Forest to the on and Off-year Management: A Case Study in Anji County, Zhejiang, China." *Forest Ecology and Management* 409: 1–7. doi:10.1016/j.foreco.2017.11.008.

Chen, X. 2010. "Discussion on the Growth Regulation of On-year and Off-year Moso Bamboo." *Central South Forest Inventory and Planning* 29 (1): 21–23. doi:10.16166/j.cnki.cn43-1095.2010.01.008.

Chen, Y., L. Li, D. Lu, and D. Li. 2019. "Exploring Bamboo Forest Aboveground Biomass Estimation Using Sentinel-2 Data." *Remote Sensing* 11 (1): 7. doi:10.3390/rs11010007.

Clevers, J. G., and A. A. Gitelson. 2013. "Remote Estimation of Crop and Grass Chlorophyll and Nitrogen Content Using Red-edge Bands on Sentinel-2 And-3." *International Journal of Applied Earth Observation and Geoinformation* 23: 344–351. doi:10.1016/j.jag.2012.10.008.

Clevers, J. G. P. W., S. M. De Jong, G. F. Epema, F. D. Van Der Meer, W. H. Bakker, A. K. Skidmore, K. H. Scholte, et al. 2002. "Derivation of the Red-edge Index Using the MERIS Standard Band Setting." *International Journal of Remote Sensing* 23 (16): 3169–3184. doi:10.1080/01431160110104647.

Dai, W., W. Fu, P. Jiang, K. Zhao, Y. Li, and J. Tao. 2018. "Spatial Pattern of Carbon Stocks in Forest Ecosystems of a Typical Subtropical Region of Southeastern China." *Forest Ecology and Management* 409: 288–297. doi:10.1016/j.foreco.2017.11.036.

Dannenberg, M. P., C. Song, T. Hwang, and E. K. Wise. 2015. "Empirical Evidence of El Niño–Southern Oscillation Influence on Land Surface Phenology and Productivity in the Western United States." *Remote Sensing of Environment* 159: 167–180. doi:10.1016/j.rse.2014.11.026.

Elmore, A. J., S. M. Guinn, B. J. Minsley, and A. D. Richardson. 2012. "Landscape Controls on the Timing of Spring, Autumn, and Growing Season Length in mid-Atlantic Forests." *Global Change Biology* 18: 656–674. doi:10.1111/j.1365-2486.2011.02521.x.

Fang, W., R. Gui, L. Ma, A. Jin, X. Lin, and X. Yu. 2015. *China Economic Bamboo*. Beijing, China: Science Press.

FAO. 2014. *State of the World's Forests 2014*. Rome, Italy: Food and Agriculture Organization of the United Nations.

Fernández-Manso, A., O. Fernández-Manso, and C. Quintano. 2016. "SENTINEL-2A Red-edge Spectral Indices Suitability for Discriminating Burn Severity." *International Journal of Applied Earth Observation and Geoinformation* 50: 170–175. doi:10.1016/j.jag.2016.03.005.

Frampton, W. J., J. Dash, G. Watmough, and E. J. Milton. 2013. "Evaluating the Capabilities of Sentinel-2 for Quantitative Estimation of Biophysical Variables in Vegetation." *ISPRS Journal of Photogrammetry and Remote Sensing* 82: 83–92. doi:10.1016/j.isprsjprs.2013.04.007.

Guyon, D., M. Guillot, Y. Vitasse, H. Cardot, O. Hagolle, S. Delzon, and J. P. Wigneron. 2011. "Monitoring Elevation Variations in Leaf Phenology of Deciduous Broadleaf Forests from SPOT/VEGETATION Time-series." *Remote Sensing of Environment* 115 (2): 615–627. doi:10.1016/j.rse.2010.10.006.

Hagolle, O., G. Dedieu, B. Mougenot, V. Debaecker, B. Duchemin, and A. Meygret. 2008. "Correction of Aerosol Effects on Multi-temporal Images Acquired with Constant Viewing Angles: Application to Formosat-2 Images." *Remote Sensing of Environment* 112 (4): 1689–1701. doi:10.1016/j.rse.2007.08.016.

Hagolle, O., M. Huc, D. V. Pascual, and G. Dedieu. 2010. "A Multi-temporal Method for Cloud Detection, Applied to FORMOSAT-2, Venµs, LANDSAT and SENTINEL-2 Images." *Remote Sensing of Environment* 114 (8): 1747–1755. doi:10.1016/j.rse.2010.03.002.

Henebry, G. M., and K. M. de Beurs. 2013. "Remote Sensing of Land Surface Phenology: A Prospectus." In *Phenology: An Integrative Environmental Science*, 385–411, edited by M. D. Schwartz. Dordrecht: Springer.

Hermance, J. F. 2007. "Stabilizing High-order, Non-classical Harmonic Analysis of NDVI Data for Average Annual Models by Damping Model Roughness." *International Journal of Remote Sensing* 28: 2801–2819. doi:10.1080/01431160600967128.

Herrmann, I., A. Pimstein, A. Karnieli, Y. Cohen, V. Alchanatis, and D. J. Bonfil. 2011. "LAI Assessment of Wheat and Potato Crops by VENµS and Sentinel-2 Bands." *Remote Sensing of Environment* 115 (8): 2141–2151. doi:10.1016/j.rse.2011.04.018.

Li, L., N. Li, D. Lu, and Y. Chen. 2019. "Mapping Moso Bamboo Forest and Its On-year and Off-year Distribution in a Subtropical Region Using Time-series Sentinel-2 and Landsat 8 Data." *Remote Sensing of Environment* 231: 111265. doi:10.1016/j.rse.2019.111265.

Liu, H., and A. R. Huete. 1995. "A Feedback Based Modification of the NDVI to Minimize Canopy Background and Atmosphere Noise." *IEEE Transaction on Geoscience and Remote Sensing* 33 (2): 457–465. doi:10.1109/TGRS.1995.8746027.

Liu, Y., C. Wu, D. Peng, S. Xu, A. Gonsamo, R. S. Jassal, M. Altaf Arain, et al. 2016. "Improved Modeling of Land Surface Phenology Using MODIS Land Surface Reflectance and Temperature at Evergreen Needleleaf Forests of Central North America." *Remote Sensing of Environment* 176: 152–162. doi:10.1016/j.rse.2016.01.021.

Ma, M., and F. Veroustraete. 2006. "Reconstructing Pathfinder AVHRR Land NDVI Time-series Data for the Northwest of China." *Advances in Space Research* 37: 835–840. doi:10.1016/j.asr.2005.08.037.

Main, R., M. A. Cho, R. Mathieu, M. M. O'Kennedy, A. Ramoelo, and S. Koch. 2011. "An Investigation into Robust Spectral Indices for Leaf Chlorophyll Estimation." *ISPRS Journal of Photogrammetry and Remote Sensing* 66 (6): 751–761. doi:10.1016/j.isprsjprs.2011.08.001.

Manivasagam, V. S., G. Kaplan, and O. Rozenstein. 2019. "Developing Transformation Functions for VENµS and Sentinel-2 Surface Reflectance over Israel." *Remote Sensing* 11 (14): 1710. doi:10.3390/rs11141710.

Melaas, E. K., M. A. Friedl, and Z. Zhu. 2013. "Detecting Interannual Variation in Deciduous Broadleaf Forest Phenology Using Landsat TM/ETM+ Data." *Remote Sensing of Environment* 132: 176–185. doi:10.1016/j.rse.2013.01.011.

Nath, A. J., R. Lal, and A. K. Das. 2015. ""Managing Woody Bamboos for Carbon Farming and Carbon Trading." *Global Ecology and Conservation* 3: 654–663. doi:10.1016/j.gecco.2015.03.002.

Pastor-Guzman, J., J. Dash, and P. M. Atkinson. 2018. "Remote Sensing of Mangrove Forest Phenology and Its Environmental Drivers." *Remote Sensing of Environment* 205: 71–84. doi:10.1016/j.rse.2017.11.009.

Roy, D. P., Z. Li, and H. K. Zhang. 2017. "Adjustment of Sentinel-2 Multispectral Instrument (MSI) Red-edge Band Reflectance to Nadir BRDF Adjusted Reflectance (NBAR) and Quantification of Red-edge Band BRDF Effects." *Remote Sensing* 9: 1325. doi:10.3390/rs9121325.

Roy, D. P., H. K. Zhang, J. Ju, J. L. Gomez-Dans, P. E. Lewis, C. B. Schaaf, Q. Sun, et al. 2016. "A General Method to Normalize Landsat Reflectance Data to Nadir BRDF Adjusted Reflectance." *Remote Sensing of Environment* 176: 255–271. doi:10.1016/j.rse.2016.01.023.

Sakamoto, T., M. Yokozawa, H. Toritani, M. Shibayama, N. Ishitsuka, and H. Ohno. 2005. "A Crop Phenology Detection Method Using Time-series MODIS Data." *Remote Sensing of Environment* 96: 366–374. doi:10.1016/j.rse.2005.03.008.

Song, X., G. Zhou, H. Jiang, S. Yu, J. Fu, W. Li, W. Wang, et al. 2011. "Carbon Sequestration by Chinese Bamboo Forests and Their Ecological Benefits: Assessment of Potential, Problems, and Future Challenges." *Environmental Reviews* 19: 418–428. doi:10.1139/a11-015.

Tucker, C. 1979. "Red and Photographic Infrared Linear Combinations for Monitoring Vegetation." *Remote Sensing of Environment* 8 (2): 127–150. doi:10.1016/0034-4257(79)90013-0.
Wu, C., A. Gonsamo, C. M. Gough, J. M. Chen, and S. Xu. 2014. "Modeling Growing Season Phenology in North American Forests Using Seasonal Mean Vegetation Indices from MODIS." *Remote Sensing of Environment* 147: 79–88. doi:10.1016/j.rse.2014.03.001.
Wu, C., D. Peng, K. Soudani, L. Siebicke, C. M. Gough, M. A. Arain, G. Bohrer, et al. 2017. "Land Surface Phenology Derived from Normalized Difference Vegetation Index (NDVI) at Global FLUXNET Sites." *Agricultural and Forest Meteorology* 233: 171–182. doi:10.1016/j.agrformet.2016.11.193.
Xie, Q., J. Dash, A. Huete, A. Jiang, G. Yin, Y. Ding, D. Peng, et al. 2019. "Retrieval of Crop Biophysical Parameters from Sentinel-2 Remote Sensing Imagery." *International Journal of Applied Earth Observation and Geoinformation* 80: 187–195. doi:10.1016/j.jag.2019.04.019.
Xu, X., H. Du, G. Zhou, F. Mao, X. Li, D. Zhu, Y. Li, et al. 2018. "Remote Estimation of Canopy Leaf Area Index and Chlorophyll Content in Moso Bamboo (Phyllostachys Edulis (Carrière) J. Houz.) Forest Using MODIS Reflectance Data." *Annals of Forest Science* 75 (1): 33. doi:10.1007/s13595-018-0721-y.
Yan, L., and D. P. Roy. 2018. "Large-area Gap Filling of Landsat Reflectance Time Series by Spectral-angle-mapper Based Spatiotemporal Similarity (SAMSTS)." *Remote Sensing* 10 (4). doi:10.3390/rs10040609.
Yang, Q., G. Yang, Q. Song, J. Shi, M. Ouyang, H. Qi, and X. Fang. 2015. "Ecological Studies on Bamboo Expansion: Process, Consequence and Mechanism." *Chinese Journal of Plant Ecology* 39 (1): 110–124. doi:10.17521/cjpe.2015.0012.
Yuen, J. Q., T. Fung, and A. D. Ziegler. 2017. "Carbon Stocks in Bamboo Ecosystems Worldwide: Estimates and Uncertainties." *Forest Ecology and Management* 393: 113–138. doi:10.1016/j.foreco.2017.01.017.
Zarco-Tejada, P. J., A. Hornero, P. S. A. Beck, T. Kattenborn, P. Kempeneers, and R. Hernández-Clemente. 2019. "Chlorophyll Content Estimation in an Open-canopy Conifer Forest with Sentinel-2A and Hyperspectral Imagery in the Context of Forest Decline." *Remote Sensing of Environment* 223: 320–335. doi:10.1016/j.rse.2019.01.031.
Zeng, L., B. D. Wardlow, D. Xiang, S. Hu, and D. Li. 2020. "A Review of Vegetation Phenological Metrics Extraction Using Time-series, Multispectral Satellite Data." *Remote Sensing of Environment* 237: 111511. doi:10.1016/j.rse.2019.111511.
Zhang, X., M. A. Friedl, C. B. Schaaf, A. H. Strahler, J. C. F. Hodges, F. Gao, B. C. Reed, and A. Huete. 2003. "Monitoring Vegetation Phenology Using MODIS Time-series Data." *Remote Sensing of Environment* 84: 471–475. doi:10.1016/S0034-4257(02)00135-9.
Zheng, Y., and W. Hong, 1998. "Moso Bamboo Management." Xiamen University Press: Xiamen, China.
Zhou, Y., G. Zhou, H. Du, Y. Shi, F. Mao, Y. Liu, L. Xu, et al. 2019. "Biotic and Abiotic Influences on Monthly Variation in Carbon Fluxes in On-year and Off-year Moso Bamboo Forest." *Trees* 33 (1): 153–169. doi:10.1007/s00468-018-1765-1.
Zhu, W., Y. Pan, H. He, L. Wang, M. Mou, and J. Liu. 2012. "A Changing-weight filter Method for Reconstructing A High-quality NDVI Time Series to Preserve the Integrity of Vegetation Phenology." *IEEE Transactions on Geoscience and Remote Sensing* 50 (4): 1085–1094. doi:10.1109/TGRS.2011.2166965.
Zhu, Z., C. E. Woodcock, C. Holden, and Z. Yang. 2015. "Generating Synthetic Landsat Images Based on All Available Landsat Data: Predicting Landsat Surface Reflectance at Any Given Time." *Remote Sensing of Environment* 162: 67–83. doi:10.1016/j.rse.2015.02.009.